

ALIGNMENT BETWEEN THE HOST AND THE NEAREST NEIGHBOR GROUPS

YOUNGANG WANG¹, CHANGBOM PARK², XIAOHU YANG^{3,4}, YUN-YOUNG CHOI⁵, XUELEI CHEN¹

Draft version November 13, 2018

ABSTRACT

We measure four different types of alignment signals using the galaxy groups of the Sloan Digital Sky Survey Data Release 4 to probe the impact of large scale environment on the distribution of satellite galaxies, on the the orientation of the central and satellite galaxies: (1) the alignment between the distributions of the satellites relative to the direction of the nearest neighbor group (NNG); (2) the alignment between the major axis direction of the central galaxy of the host group (HG) and the direction of the NNG; (3) the alignment between the two major axes of the central galaxies of the HG and NNG; and (4) the alignment between the major axes of the satellites of the HG and the direction of the NNG. We find strong alignment signals of satellite distribution and orientation of central galaxy relative to the direction of the NNG even when the NNG locates beyond $3r_{\text{vir}}$ of the host group. The alignment signals are stronger for groups that are more massive and with early type central galaxies. For the orientation of satellite galaxies, however, we do not find any significant alignment signals relative to the direction of the NNG. From these four types of the alignment measures, we conclude that the large scale environment traced by the nearby group mainly impacts the shape of the host dark matter halo, hence impacts the distribution of satellite galaxies and the orientation of central galaxies. Apart from these, there is additional impacts by the large scale environment directly onto the distribution of satellite galaxies.

Subject headings: methods: statistical-galaxies: haloes-galaxies: structure-dark matter-large scale structure of universe

1. INTRODUCTION

The distribution of satellites in the groups of galaxies holds important clues to the assembly history of dark matter halos. Since satellite galaxies are typically distributed over the entire dark matter halo, they are a useful tracer of the dark matter distribution on the scale of individual dark matter halos. In particular, their positional information can be used to determine the shape of the dark matter haloes (Carter & Metcalfe 1980; Plionis, Barrow & Frenk 1991; Fasano et al. 1993; Basilakos, Plionis & Maddox 2000; Orlov, Petrova & Martynova 2001; Plionis et al. 2004, 2006; Bailin & Steinmetz 2005; Wang et al. 2008, hereafter W08), and their kinematics can provide estimates of the dynamical mass of the haloes (e.g., Zaritsky et al. 1993, 1997; McKay et al. 2002; Brainerd & Specian 2003; Katgert et al. 2004; van den Bosch et al. 2004). Therefore, it is important to have an precise quantitative description of the distribution of satellite galaxies with respect to the host dark halos.

One way to describe the distribution of satellites in the groups of galaxies is to measure the alignment between the spatial distribution of satellite galaxies in groups and the orientation of their central galaxies. Since Holmberg (1969) found that satellites are preferentially located along the minor axis of isolated disc galaxies, there

have been extensive studies with high resolution simulations (Knebe et al. 2004, 2008; Libeskind et al. 2005; Wang et al. 2005; Zentner et al. 2005; Kang et al. 2007) and observations (Hawley & Peebles 1975; Lynden-Bell 1976, 1982; Sharp, Lin & White 1979; MacGillivray et al. 1982; Majewski 1994; Hartwick 1996, 2000; Zaritsky et al. 1997; Kroupa et al. 2005; Brainerd 2005; Koch & Grebel 2006; McConnachie & Irwin 2006; Yang et al. 2006 (hereafter Y06); Metz et al. 2007; W08; Steffen & Valenzuela 2008) on this subject. These studies have focused on whether the satellites are distributed along the major axis or minor axis of the central galaxy. It is believed that the origin of this satellite-host alignment is the anisotropic distribution of the satellites in the dark matter halo. The anisotropy can be strengthened by the tidal forces from the host halo (e.g., Ciotti & Dutta 1994; Usami & Fujimoto 1997; Fleck & Kuhn 2003), but can be significantly weakened due to some nonlinear effects such as violent relaxation and encounters (e.g., Porciani et al. 2002).

Besides the alignment between the distribution of satellite galaxies and the orientation of their central galaxy, there are also some other forms of alignment which have been investigated. The alignment between neighboring clusters (Binggeli 1982; West 1989; Plionis 1994), between brightest cluster galaxies (BCGs) and their parent clusters (Carter & Metcalfe 1980; Binggeli 1982; Struble 1990), between the orientation of satellite galaxies and the orientation of the cluster (Dekel 1985; Plionis et al. 2003), and between the orientation of satellite galaxies and the orientation of the BCG (Struble 1990). Using the same group catalogue as that used here, Faltenbacher et al. (2007) examined the three different types of intrinsic galaxy alignment within groups: halo alignment between the orientation of the brightest

¹ National Astronomical Observatories, Chinese Academy of Sciences, Beijing 100012, China; E-mail: wangyg@bao.ac.cn

² Korea Institute for Advanced Study, Dongdaemun-gu, Seoul 130-722, Korea; cbp@kias.re.kr

³ Shanghai Astronomical Observatory, the Partner Group of MPA, Nandan Road 80, Shanghai 200030, China

⁴ Joint Institute for Galaxy and Cosmology (JOINGC) of Shanghai Astronomical Observatory and University of Science and Technology of China

⁵ Astrophysical Research Center for the Structure and Evolution of the Cosmos, Sejong University, Seoul 143-747, Korea

group galaxies (BGG) and the distribution of its satellite galaxies, radial alignment between the orientation of a satellite galaxy and the direction toward its BGG, and direct alignment between the orientation of the BGG and that of its satellites. Their results have subsequently been confirmed by their simulation studies (Faltenbacher et al. 2008).

In this paper, we aim to study the effects of the large scale environment on the various properties of the central and satellite galaxies, i.e., on the distribution of satellite galaxies, on the shapes of the central and satellite galaxies. In our approach the large scale environment is characterized by the nearest neighbor groups (hereafter NNG). For our purposes, the following alignment signals are measured: (1) the alignment between the distributions of the satellites relative to the direction of the NNG; (2) the alignment between the major axis of the central galaxy of the host group (HG) and the direction of the NNG; (3) the alignment between the two major axes of the central galaxies of the HG and the NNG; and (4) the alignment between the major axes of the satellites of the HG and the direction of the NNG. Here the alignment signals (2), (3) and (4) are measured to probe the impact of the large scale environment on the shapes of the central and satellite galaxies, respectively.

This paper is organized as follows. In Section 2, we briefly describe the observational data used for this study. Section 3 presents the method to quantify the alignment signal. Section 4 shows the results of various kinds of alignment signals we measured from the SDSS and their dependence on the morphology of the central galaxies of the HG and the NNG. Section 5 presents a summary and discussion.

2. OBSERVATIONAL DATA SET

2.1. Groups: central and satellite galaxies

The analysis presented in this paper is based on the SDSS DR4 galaxy group catalogue of Yang et al. (2007). This group catalogue is constructed by applying the halo-based group finder of Yang et al. (2005) to the New York University Value-Added Galaxy Catalogue (NYU-VAGC; see Blanton et al. 2005), which is based on SDSS DR4 (Adelman-McCarthy et al. 2006). From this catalogue Yang et al. selected all galaxies in the Main Galaxy Sample with redshifts in the range $0.01 \leq z \leq 0.20$ and with a redshift completeness greater than 0.7. This sample of galaxies is further divided into three group samples: sample I, which only uses the 362,356 galaxies with measured redshifts from the SDSS; sample II, which also includes 7091 galaxies with SDSS photometry but with redshifts taken from alternative surveys; and sample III, which includes an additional 38,672 galaxies that lack a redshift due to fiber-collisions, but was assigned the redshift of its nearest neighbor (cf. Zehavi et al. 2002). The present analysis is based on the sample II which consists of 369,447 galaxies distributed over 301,237 groups with a sky coverage of 4514 deg^2 . Details of the group finder and the general properties of the groups can be found in Yang et al. (2007).

The halo mass of each group is estimated using the ranking of group's characteristic stellar mass, M_{stellar} , defined as the total stellar masses of all group members with $^{0.1}M_r - 5 \log h \leq -19.5$. More details of the mass

estimations can be found in Yang et al. (2007). For those groups with all members that have absolute magnitudes $^{0.1}M_r - 5 \log h > -19.5$, which are not assigned halo masses in the group catalogue, we use the mean stellar-to-halo mass relation obtained in Yang et al. (2008) to assign their halo masses. In this study, only groups with halo masses $M \geq 10^{11.5} h^{-1} M_{\odot}$ are selected. Note also that in these group catalogues the survey edge effects have been taken into account (Yang et al. 2007). We use only those groups with $f_{\text{edge}} \geq 0.6$, where $1 - f_{\text{edge}}$ is the fraction of galaxies in a group that are missed due to the survey edges.

Applying all the above mentioned selection criteria, we have a total of 27,173 central galaxies and 64,366 satellite galaxies. Here the central galaxy is defined to be the most massive (in terms of stellar mass) galaxy in each group and other galaxies are satellites. In order to study the shape related properties of galaxies, only galaxies with $b/a < 0.75$ are selected so that their orientations are well defined. Here a and b are the isophotal semi-major and minor axis lengths, respectively. The isophotal position angle is used to define the orientation of the galaxy. For this purpose, 13,890 central galaxies and 44,219 satellite galaxies are selected.

Finally, note that the selected galaxy groups contain some interlopers, i.e. false members assigned to a group. If the distribution of these interlopers is uncorrelated (or anti-correlated) with that of the true members of the group, our results on the first kind of alignment would be negatively biased. According to Yang et al. (2007; 2005) the average fraction of interlopers in the group is less than 20%. We have tested the effects of such interlopers by assuming that the distribution of the interlopers is uncorrelated with the shape of the group and is spherical, and found that the presence of the interlopers can decrease the first type of the alignment signal by $\sim 10\%$.

2.2. Galaxies: early and late types, position angles

In our study we follow the prescription of Park & Choi (2005) to divide our sample into the early (ellipticals and lenticulars) and the late (spirals and irregulars) morphological types. This division is based on their location in the $u - r$ versus $g - i$ color gradient space, and also in the i -band concentration index space. The early type galaxies are classified as those lying above the boundary lines passing through the points (3.5, -0.15), (2.6, -0.15), and (1.0, 0.3) in the $u - r$ versus $\Delta(g - i)$ space. They are also required to have the (inverse) concentration index $c \equiv R_{50}/R_{90} < 0.43$, where R_{50} and R_{90} are the radii from the center of galaxy containing 50% and 90% of the Petrosian flux. The rest of the galaxies are classified as late-type galaxies. The completeness and reliability of this classification scheme reaches 90%. For more details of the morphology classification, we refer the reader to Park & Choi (2005). In this paper, we adopt the r band isophotal position angle for each galaxy, which is given in the SDSS-DR4 (Adelman-McCarthy et al. 2006). We have checked the distributions of these position angles and found them to be isotropic.

2.3. The nearest neighbor group

A very important steps in our investigation is to find the nearest neighbor group, so that we can define/estimate the direction of the tidal force. For a given

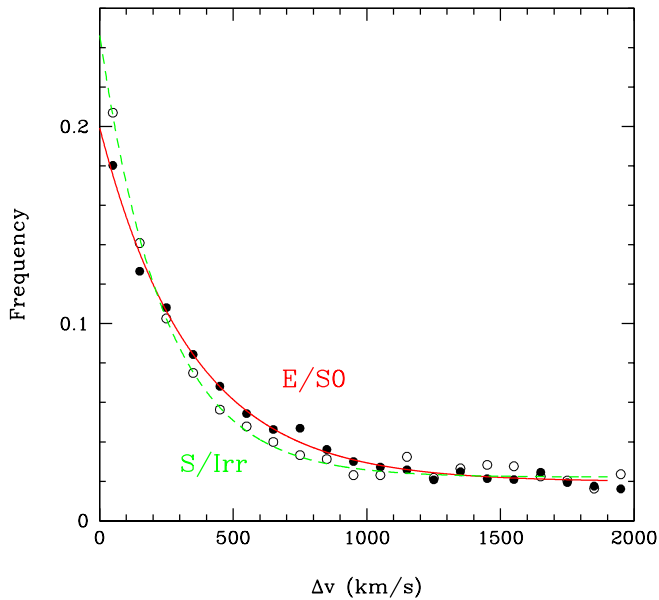


FIG. 1.— Probability distribution of the velocity difference Δv between early (filled dot) or late (open circle) type centrals and other central galaxies at projected separation $r_p = 0.4 \sim 1 h^{-1} \text{Mpc}$. The solid line is the best fit curve for the early (E/S0) morphological type centrals, while the dashed one is for the late (S/Irr) type centrals.

host group, its NNG is found in the following way. To select the closest neighbor we combine the pairwise velocity differences and the projected distances between the central galaxies of the HG and its neighboring groups. To find the velocity difference criteria we first inspect the distribution of the pairwise velocity difference between central galaxies of the HG and the neighboring groups. Figure 1 shows the distribution of the velocity difference Δv for the early (filled dot) and late (open circle) type centrals. These profiles are obtained from the projected distance r_p between 0.4 and $1 h^{-1} \text{Mpc}$. We found that the observed velocity difference profile is far from Gaussian, so we used an exponential plus a constant model to fit these profiles, and obtained the characteristic velocity differences of 342 and 243 km/s for early and late type centrals respectively. The fitting curves are shown as the solid (early type) and dashed (late type) lines in Figure 1.

We then have the following criteria to select the NNG: (1) for a given central galaxy of a HG, the central galaxy of the neighbor group should have velocity difference less than 800 (for early type centrals) or 600 (for late-type centrals) km/s (about 2.4 times the characteristic velocity differences) and projected separation $r_p < 3 h^{-1} \text{Mpc}$. The neighbor with the smallest r_p is the NNG; (2) if there is no central galaxy within the velocity and r_p volume, the neighbor with the smallest three dimensional separation is the NNG.

Finally, note that one can also define the NNG according to the project separation relative to the size of the host group (e.g., its virial radius). However, as we have tested, using such an alternative definition of the NNG will not impact any of our results significantly.

3. QUANTIFYING THE ALIGNMENT

In order to probe the impacts of the large scale environment on the various properties of the central and

satellite galaxies, we first measure the different alignment signals as we listed in Section 1. The alignments of objects are obtained by computing the distribution functions of the alignment angles (e.g., Brainerd 2005), $P(\theta_i)$ ($i = 1, 2, 3, 4$), where θ_i is the angle between the two directions.

The angle θ_1 is the projected angle between the central-satellite direction and the direction of the NNG (See the left panel of Figure 2). The angle θ_1 is constrained in the range $0^\circ \leq \theta_1 \leq 180^\circ$, where $\theta_1 < 90^\circ$ ($> 90^\circ$) implies a satellite is at the near (far) side of the HG with respect to the NNG.

The angle θ_2 is the angle between the major axis of the central galaxy of the HG and the direction of the NNG (See the left panel of Figure 2), which is constrained to be in the range $0^\circ \leq \theta_2 \leq 90^\circ$. $\theta_2 = 0^\circ$ (90°) suggests that the major (minor) axis of the central galaxy of the HG is perfectly aligned with the direction of the NNG.

The angle θ_3 is the angle between the two major axes of the central galaxies of the HG and the NNG. Since there is no good way to globally define the angle between two angles at different locations of the celestial sphere, we use the parallel transport of the angles along the great circles, which can be explained by the right panel of Figure 2 and in the Appendix. The angle θ_3 is also constrained in the range $0^\circ \leq \theta_3 \leq 90^\circ$.

The angle θ_4 is similar to θ_2 but defined for the major axes of the satellite galaxies, i.e., the angle between the major axis of the satellite galaxy of the HG and the direction of the NNG.

In the following we will take θ_1 as an example to explain the process of measuring the alignment signals, the measurement of $\theta_2, \theta_3, \theta_4$ are similar. For a given set of the HG-NNG pairs, we first count the number of satellite-central-NNG pairs, $N(\theta_1)$, that have the angle θ_1 between the central-satellite direction and the direction of the NNG in a number of θ_1 bins. Next, we construct 100 random samples in which we randomize the positions of all NNGs, and compute $\langle N_R(\theta_1) \rangle$, the average number of satellite-central-NNG pairs for randomly located NNGs as function of θ_1 . Note that this ensures the random samples have exactly the same selection effects as the real sample, so that any significant difference between $N(\theta_1)$ and $N_R(\theta_1)$ reflects a genuine alignment between the distribution of the satellite galaxies in the HG and the direction of the NNG.

To quantify the strength of any possible alignment we follow Y06 and W08 and define the distribution of normalized pair counts:

$$f_{\text{pairs}}(\theta_1) = \frac{N(\theta_1)}{\langle N_R(\theta_1) \rangle}. \quad (1)$$

Note that in the absence of any alignment, $f_{\text{pairs}}(\theta_1) = 1$, while $f_{\text{pairs}}(\theta_1) > 1$ near $\theta = 0$ or 180 degree implies a satellite distribution aligned along the direction of the NNG. We use $\sigma_R(\theta_1) / \langle N_R(\theta_1) \rangle$, where σ_R is the standard deviation of $N_R(\theta)$ obtained from the 100 random samples, to assess the significance of the deviation of $f_{\text{pairs}}(\theta_1)$ from unity. In addition to this normalized pair count, we also compute the average angle $\langle \theta_1 \rangle$. Note that in case of the angles θ_1 that are constrained in the range $0^\circ \leq \theta_1 \leq 180^\circ$, we first convert the angles into the range $0^\circ \leq \theta_1 \leq 90^\circ$ using $\theta_1 \rightarrow 180^\circ - \theta_1$ (if $\theta_1 > 90^\circ$). In the absence of any alignment $\langle \theta_1 \rangle = 45^\circ$,

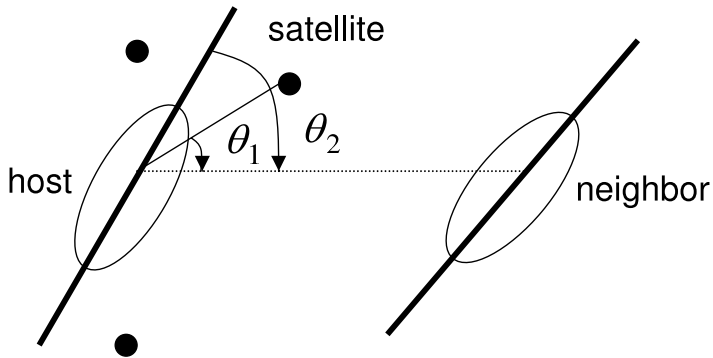


FIG. 2.— Illustration of the first three alignment angles θ_1 , θ_2 (left panel) and θ_3 (right panel).

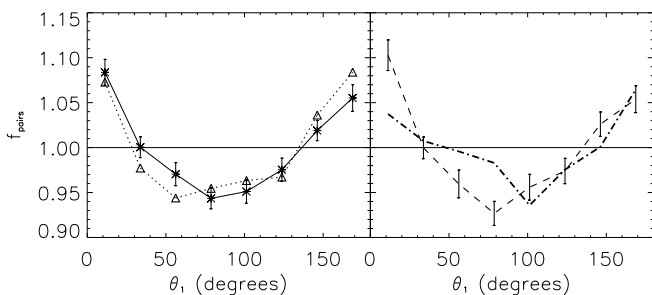


FIG. 3.— The normalized probability distribution, $f_{\text{pairs}}(\theta_1)$, of the angle θ_1 . Here θ_1 is the angle between the directions of the satellite galaxies in the HG and the NNG. In the left panel, we show results for the whole sample (solid line) and the subsample with projected distance smaller than 3 times of the virial radius of the host group (dotted line). In the right panel, we show results for subsamples where the mass of the HG are larger (smaller) than that of the NNG with dashed (dot-dashed) line.

and $\langle \theta_1 \rangle < 45^\circ$ ($\langle \theta_1 \rangle > 45^\circ$) means that the satellites are parallel (perpendicular) to the line connecting the host-neighbor pairs.

4. RESULTS

4.1. Satellite galaxy distribution relative to the direction of the NNG

As have been found in recent papers, the satellite galaxies are distributed preferentially along the major axis of the central galaxies in halos of different masses, especially those with red central galaxies (e.g., Brainerd 2005; Agustsson & Brainerd 2006; Y06; Azzaro et al. 2007; Kang et al. 2007; W08). This shows that the distributions of the satellite galaxies are not completely spherical, and are correlated with the shapes of the central galaxies. In this subsection we check whether such a correlation also holds beyond the size of dark matter halos.

The left-hand panel of Figure 3 shows the alignment between the orientation of the satellite system in the HG and the direction of the NNG calculated from all satellite-NNG pairs (solid line) in our SDSS group catalogue. One can see that $f_{\text{pairs}}(\theta_1) > 1$ at small (near 0°) and large θ_1 (near 180°) values, while it is less than 1 at middle values (near 90°). This clearly indicates that the satellites of HG are distributed preferentially along the direction of the NNG. Apparently, there is a significant large scale environmental effect (due e.g. to filaments) on the dis-

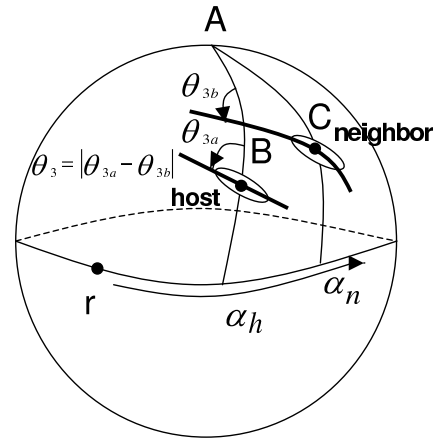


FIG. 4.— Similar to Fig. 3, but here for different HG-NNG systems. Left panel: results for HG-NNG systems where the mass of the HG is larger than that of the NNG. Right panel: results for HG-NNG systems where the mass of the HG is smaller than that of the NNG. In each panel, the solid, dotted and dashed lines represent the mass of the NNG in the range $M_n \in [11.5, 12.5]$, $[12.5, 13.5]$ and $[13.5, 14.5]$, respectively

tribution of satellite galaxies along the direction of the NNG. For comparison, the dotted line in the left panel of Figure 3 shows $f_{\text{pairs}}(\theta_1)$ for the host-neighbor pairs with the projected distance smaller than 3 times of the virial radius of the HG. There is no significant difference between the solid and dotted lines. In other words, the closest neighbor (or large scale environment, e.g. the filament) can affect the distribution of the satellites even if the neighbor is farther than three times the virial radius of the HG. Note that in our HG-NNG systems, the NNG can be either more massive or less massive than the HG, and it may be interesting to investigate these two cases separately. For this purpose, in the right-hand panel of Figure 3 we show the resulting θ_1 distributions for HG-NNG systems with the mass of HG larger (dashed line) and smaller (dot-dashed line) than that of the NNG⁶. It is quite clear that the distribution of satellite galaxies in more massive host group is more strongly affected by or correlated with the large scale environment.

We can further check this by measuring the alignment signals for HG-NNG systems that are divided into subsamples of different masses. In the left panel of Fig-

⁶ In what follows, unless stated otherwise, we use solid line to represent the sample which is not constrained by the distance limit, while the dotted one to represent the results with the projected distance smaller than 3 times the virial radius of the HG; the dashed (dot-dashed) line represents the results for subsamples where the mass of the HG are larger (smaller) than that of the NNG in the rest part of the paper.

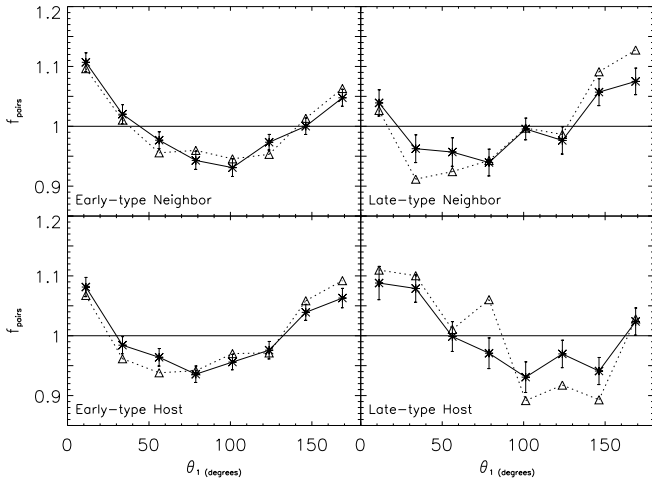


FIG. 5.— Same as Fig. 3, but for different subsamples, divided by the type of the central galaxies of the HG or NNG.

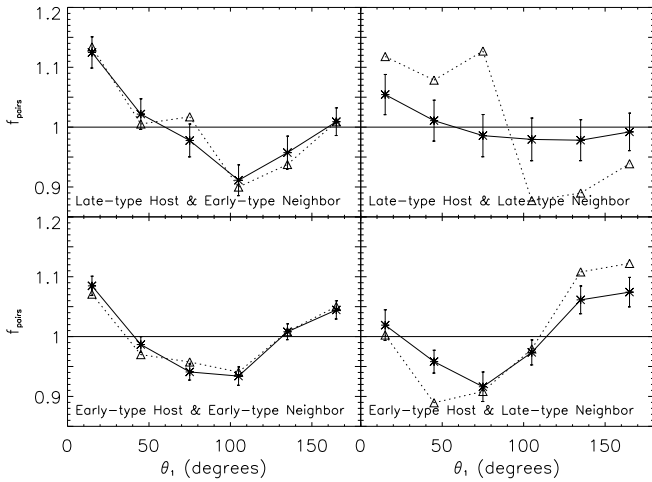


FIG. 6.— Same as Fig. 5, except that here we split the sample according to the morphological types of both the central galaxies of the HG and NNG.

ure 4, we show the alignment signal of $f_{\text{pairs}}(\theta_1)$ for the submaples with mass of the HG that are larger than that of the NNG, while in the right panel of the Figure 4, we show the results of the subsamples with the mass of the HG smaller than that of the NNG. In each panel, the solid, dotted and dashed lines represent the mass of the NNG in the range $M_n \equiv \log_{10}(hM/M_\odot) \in [11.5, 12.5]$, $[12.5, 13.5]$ and $[13.5, 14.5]$, respectively. We found some interesting trends here. According to the left panel of Fig. 4, for the most massive groups ($M_n > 13.5$), the alignment signal (i.e. deviation of $f_{\text{pairs}}(\theta_1)$ from 1) is strong, perhaps indicating that the large scale environment (e.g. filament) is at action. For system with less massive HG and NNGs ($M_n \in [12.5, 13.5]$), the signal is weaker. However, for the smallest groups discussed here ($M_n \in [11.5, 12.5]$), the alignment signal is again rather strong. Interestingly, for those systems with NNG heavier than HG (right panel), there are slightly more satellite galaxies distributed near the NNG (with $\theta_1 < 90^\circ$) than HG, which may indicate that the NNG near a small HG may attract its satellite galaxies and affect their distribution.

In order to study how this alignment depends on the morphological types of the central galaxies of the HG

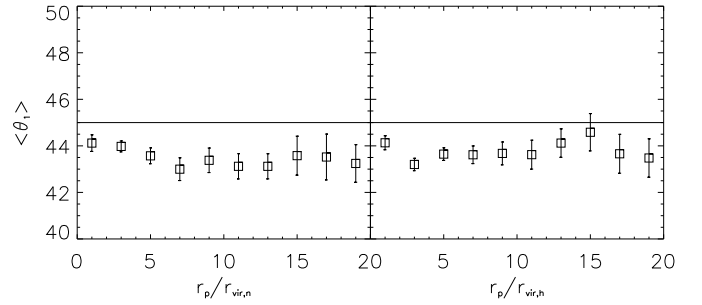


FIG. 7.— The average value of θ_1 as a function of the projected distance between the HG and the NNG. Left: as a function of $r_{\text{vir},n}$; Right: as a function of $r_{\text{vir},h}$.

and the NNG, following Y06 and W08, we divide our sample of host and neighbor groups into different morphology subsamples. Figure 5 shows the alignment signals $f_{\text{pairs}}(\theta_1)$ for HG with early (lower-left panel) and late-type (lower-right panel) central galaxy, and NNG with early (upper-left panel) and late-type (upper-right panel) central galaxy, respectively. The alignment signal does seem to depend on the morphological type of the central galaxy slightly: the groups with early type central galaxies or with the NNGs having an early central galaxy show slightly stronger alignment than those with late-type centrals. In Figure 6, we show the alignment, $f_{\text{pairs}}(\theta_1)$, for four combinations of the HG and NNG with central galaxies of different morphological types. As one can see, pairs with the late-type HG and late-type NNG show the smallest strength of the alignment signal.

Apart from the strength of the alignment signals, we can find that the satellite distribution in the HG is also slightly asymmetric with respect to the near side or far side from the NNG. There is a small but significant preference for the satellite galaxies in a group with a late type central galaxy to be distributed near the side of the NNG, with either an early or a late type central galaxy. The trend is even stronger for the cases where the NNG with projected separation is smaller than 3 times of the virial radius. For the groups with an early type central galaxy, however, the trend is opposite: the satellite galaxies are preferentially distributed on the far side from the NNG, again this effect is small but quite significant. The reason for this may be due to (i) the groups with late type central galaxy is more probably located in the outskirts of a high density region with groups having preferentially early type central galaxies; (ii) probably smaller than groups with early type central galaxies, thus have smaller impact on its NNG.

To study to what extent the large scale environment represented by the NNG affects the distribution of the satellite galaxies in the HG, we divided the total sample into subsamples according to the projected distance between the HG and the NNG. Figure 7 shows the dependence of the average value θ_1 on the projected distance between the HG and the NNG. Here we take both the virial radius of the NNG, $r_{\text{vir},n}$ (left panel), and the HG,

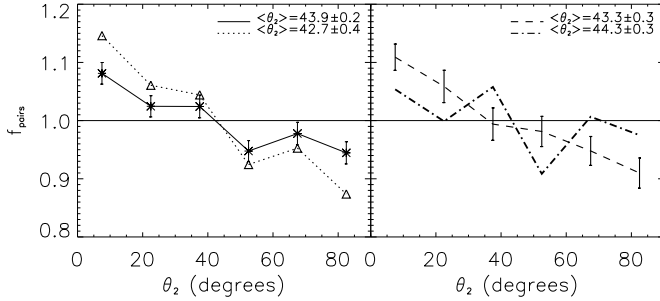


FIG. 8.— The normalized probability distribution, $f_{\text{pairs}}(\theta_2)$, of the angle θ_2 between the major axes of the central galaxy of the HG and the direction of the NNG. In the left panel, results are measured for all samples (solid line) and the subsamples with the projected distance smaller than 3 times the virial radius of the host group (dotted line). In the right panel, we show results for subsamples where the mass of the HG are larger (smaller) than that of the NNG with dashed (dot-dashed) line.

$r_{\text{vir,h}}$ (right panel), as the unit. There is no significant difference between the results in the left and right panels. The value of $\langle\theta_1\rangle$ depends weakly on the distance between the HG and NNG. The alignment between the distribution of satellite galaxies and the direction of the NNG is significant (greater than 1σ) up to separations as large as about $12r_{\text{vir,n}}$ (or $r_{\text{vir,h}}$), which is also evident from the fact that $\langle\theta_1\rangle = 43.1^\circ \pm 0.5^\circ$ (or $43.6^\circ \pm 0.6^\circ$) for the systems with separation of the HG and the NNG being $12r_{\text{vir,n}}$ (or $r_{\text{vir,h}}$).

4.2. The position angle of the central galaxy

4.2.1. relative to the direction of the NNG

Both Y06 and W08 found that there is a preference for the satellites to be distributed along the major axis of their central galaxy, and in the previous section, we found a prominent alignment between the orientation of the satellite system of the HG and the direction of the NNG. Therefore, we expect there is also an alignment between the major axis of the central galaxy of the HG and the direction of the NNG.

Indeed, as shown in the left panel of Figure 8, there is a strong signal of alignment between these two directions: the major axis of the central galaxy of the HG is preferentially aligned with the direction of the NNG. The alignment signal is even stronger for the pairs with smaller projected separations as shown by the dotted line of Figure 8. This result suggests that the major axis of the central galaxy of the HG tends to be aligned with the large scale structure (e.g., the filament) as represented by the direction of the NNG. This is also evident from the fact that $\langle\theta_2\rangle = 43.9^\circ \pm 0.2^\circ$ ($\langle\theta_2\rangle = 42.7^\circ \pm 0.4^\circ$ for the close pairs), which deviates from the case of no alignment (i.e. $\langle\theta_2\rangle = 45^\circ$ by 5σ (or 6σ)). In the right-hand panel of Figure 8 we show the resulting θ_2 distributions for HG-NNG systems with the mass of HG larger (dashed line) and smaller (dot-dashed line) than that of the NNG. It is quite clear that the position angle of the central galaxy in more massive host group is slightly more aligned and

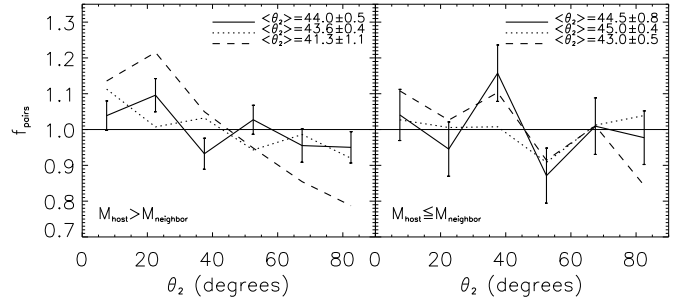


FIG. 9.— Similar to Fig. 8, but here for different HG-NNG systems. Left panel: results for HG-NNG systems where the mass of the HG is larger than that of the NNG. Right panel: results for HG-NNG systems where the mass of the HG is smaller than that of the NNG. In each panel, the solid, dotted and dashed lines represent the mass of the NNG in the range $M_n \in [11.5, 12.5]$, $[12.5, 13.5]$ and $[13.5, 14.5]$, respectively.

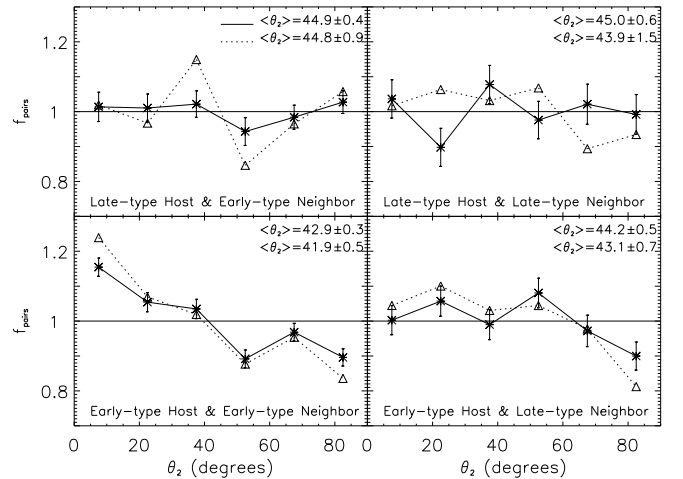


FIG. 10.— Same as Figure 8, but for different subsamples of central galaxies of the host and neighbor groups.

affected by the large scale environment.

To check on what mass scale such an alignment signal reaches its maximum, we divide our sample into subsamples of three mass bins as in Section 4.1. As shown in Figure 9, the alignment signal in the systems with the more massive HG is stronger than in the system with the lower mass of the HG. For the systems with the mass of the NNG between $10^{11.5}$ and $10^{12.5} h^{-1}M_\odot$ (and HG is even less massive), the strength of the alignment signal is no longer significant relative to the null hypothesis $\langle\theta_2\rangle = 45^\circ$ at $1\text{-}\sigma$ level for our sample.

In Figure 10, we examine how $f_{\text{pairs}}(\theta_2)$ depends on the morphological types of the central galaxies. Note that the position angles of the early types which are dominantly ellipticals, can represent quite well the orientation of the stellar distribution of the central galaxies, while the position angles of the late types which are dominantly the spirals, are very sensitive to the inclination of the galaxies, thus one would expect quite different alignment signals $f_{\text{pairs}}(\theta_2)$ for the early and late type galaxies. In the bottom two panels of Fig. 10, we show the

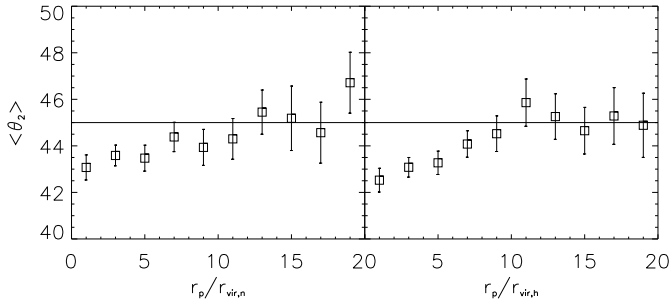


FIG. 11.— The average value of θ_2 as a function of the projected distance between the HG and the NNG. Left: as a function of $r_{vir,n}$; Right: as a function of $r_{vir,h}$.

alignment signals $f(\theta_2)$ for the early type central galaxy of the HG (lower left: NNG with early type central, lower right: NNG with late type central). It is obvious that there is a quite strong alignment signal between the position angle of the early type central galaxy in the HG with the direction of the NNG, especially if the central galaxy of the NNG is also an early type one. If the central galaxy of the NNG is a late type one, the alignment signal weakens considerably. Comparing the solid lines with the dotted lines, we can also see that the alignment strength is weakened if the NNG at larger projected separation is added.

In the case where the central galaxy of the NNG is a late type one, the major axis of the galaxy is not so well correlated with its stellar distribution, but more with the inclination of the disk. On the other hand, the minor axis is quite well correlated with the disk spin axis. Thus $\theta_2 = 0$ means that the spin axis is perpendicular to the direction of the NNG, while $\theta_2 = 90^\circ$ means that the spin axis tends to be aligned with the direction of the NNG. In the upper panels of Figure 10, we show the distribution $f(\theta_2)$ for the late type central galaxies (upper-left: NNG with early type central, upper-right: NNG with late type central). We do not find any significant alignment signal between the major axis of the central late type galaxy and the direction of the NNGs.

The alignment angle $\langle \theta_2 \rangle$ increases slowly and approaches the null position of 45° as the distance between the HG and NNG increases (See Fig. 11).

4.2.2. relative to the orientation of the central galaxy of the NNG

In Figure 12, we present the distribution of the angle θ_3 between the major axes of the central galaxy of the HG and the central galaxy of the NNG. In the lower panels we use only the HG and NNG whose central galaxies are both early types. One can see that the major axes of the central galaxies of the HG and the NNG tend to be parallel, though the signal is weak. We also checked the case of alignment between all types of central galaxies, and find there is no prominent signal, as shown by the fact $\langle \theta_3 \rangle = 44.6^\circ \pm 0.3^\circ$. However, the θ_3 alignment signal for the case of the HG more massive than the NNG is stronger than the opposite case (see the lower-right

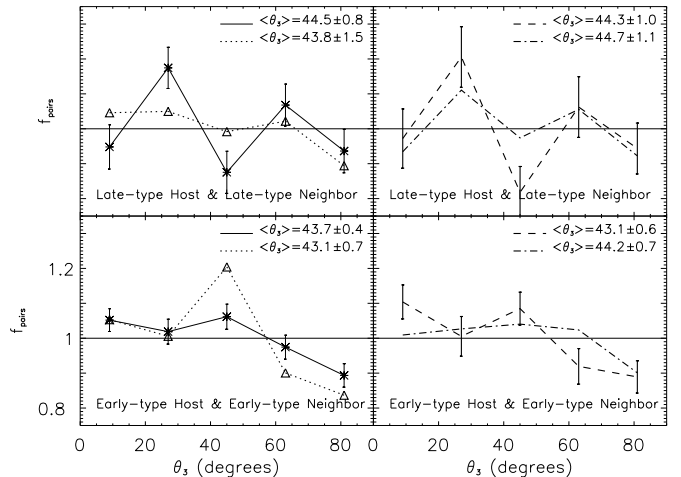


FIG. 12.— The normalized probability distribution, $f_{\text{pairs}}(\theta_3)$, of the angle θ_3 between the two major axes of the central galaxies of the HG and the NNG. Upper panels: the central galaxies of the HG and NNG are both late types. Lower panels: the central galaxies of the HG and NNG are both early types. In the two left panels we show results for all sample (solid line) and the subsample with the projected distance smaller than 3 times the virial radius of the host group (dotted line). While in the two right panels, we show the results for subsamples where the mass of the HG are large (smaller) than that of the NNG with dashed (dot-dashed) line.

panel).

The upper panels of Figure 12 shows the distributions of θ_3 when the morphological types of the central galaxies of the HG and NNG are both late types. The spin axis of the two galaxies are parallel for $\theta_3 = 0^\circ$ and perpendicular if $\theta_3 = 90^\circ$. We find large fluctuations in the distribution, and there is no significant alignment signal between the spin axes of the late-type central galaxies, regardless whether the HG is more massive or less than the NNG.

4.3. The position angle of the satellite galaxy relative to the direction of the NNG

Many studies have attempted to detect the alignment signal between the orientations of central galaxies and satellite galaxies in the clusters of galaxies (e.g., Plienis et al. 2003; Strazzullo et al. 2005; Torlina et al. 2007), most of them found only null or weak signal. Using a sample of 4289 host-satellites pairs from the SDSS DR4, Agustsson & Brainerd (2006) found a weak signal of the alignment. Adopting the same group catalogue as that used here, Faltenbacher et al. (2007) searched for the alignment between the orientations of the BGG and the satellites. They considered the total sample and submaples with different color of the satellite galaxy, and found a weak but definite alignment signal between the major axes of the central and the satellite galaxies of the host group, especially at small scales $r_p < 0.1 r_{vir,h}$, where one expects a strong tidal force at such small separation.

As we have already noticed, the large scale environment traced by the direction of the NNG can affect the distribution of satellite galaxies in the HG. Here, we check if the large scale environment can also impact the orientation of the satellite galaxies. The method to obtain the alignment angle θ_4 is similar to that for the angle θ_3 , the only difference is that here we use the major axes of the satellites to substitute the major axis of the central galaxy of the HG. Fig. 13 shows the alignment between

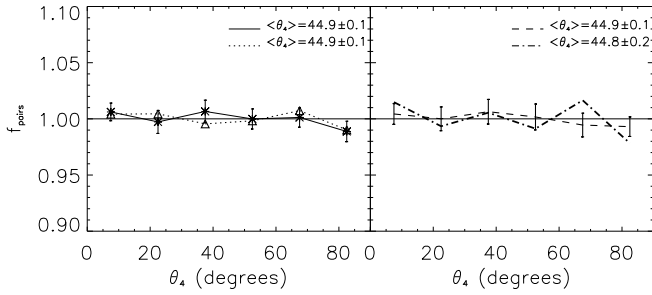


FIG. 13.— The normalized probability distribution, $f_{\text{pairs}}(\theta_4)$, of the angle θ_4 between the orientations of the satellite galaxy in HG and the direction linking the host and NNG. In the left panel, results are measured for all sample (solid line) and the subsample with the distance limit, 3 times the virial radius of the host group (dotted line). In the right panel, we show results for subsamples where the mass of the HG are large (smaller) than that of the NNG with dashed (dot-dashed) line.

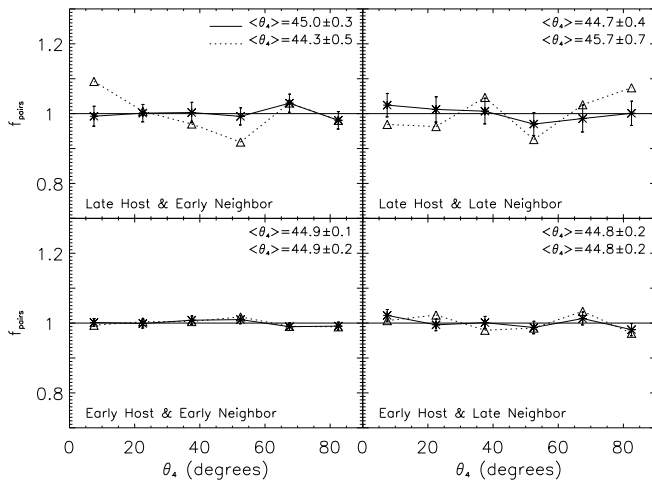


FIG. 14.— Same as Figure 13, but for different subsamples of central galaxies of the host and neighbor groups.

the major axes of the satellites in the HGs and the direction linking the host and NNGs. It is seen that there is apparently no alignment between the major axes of the satellite and the direction linking the host and the NNG. Fig 14 displays the dependence on the $f_{\text{pairs}}(\theta_4)$ on the morphological type of the central galaxies of the HGs and NNGs. We again do not find any statistically significant alignment signal for the morphology subsamples. Moreover, we also checked the distribution $f_{\text{pairs}}(\theta_4)$ separately for the early and late type satellite galaxies, and again there is no significant alignment signal.

5. SUMMARY AND DISCUSSION

In the cold dark matter scenario, small dark matter halos form first and grow subsequently to larger structures via accretion and merger processes. The accretion of material might preferentially occur along the filamentary structure (West 1994), which leads to correlations between the internal structures of the neighboring groups. Binggeli (1982) pioneered the studies of the alignment between neighboring clusters of galaxies, and found that the host clusters tend to be aligned with their nearest neighbors. The subsequent studies confirmed this tendency, although conflicting results appeared occasionally in the literature (West 1989; Plionis 1994). In this paper, we used the host-neighboring group systems extracted

from the SDSS DR4 group catalogue (Yang et al. 2007) to probe the impact of the large scale environment (as represented by the nearest neighboring group) on the distribution of the satellite galaxies and on the orientation of the central and satellite galaxies. For this purpose, four types of alignment signals are measured. The main results of this paper are summarized as follows.

1. There is a strong alignment signal between the distribution of the satellites relative to the direction of the NNG. For the system with both early central galaxies of the HG and NNG, the alignment signal is the strongest, for the system with both late central galaxies, the signal is weaker but still quite significant.
2. The satellite galaxies in the HG have a slight but statistically significant preference to be distributed at the near side of the NNG with an early type central galaxy, and at the far side of the NNG with a late type central galaxy.
3. The major axis of the central galaxy of the HG is aligned with the direction of the NNG, especially in the massive HGs, which indicates that the large scale environment (e.g. filament) can affect or be correlated with the shape of the central galaxy. This effect from the NNG is stronger for the systems when the central galaxies of HG and NNG are both early types.
4. The distribution of the satellite galaxies and the orientation of the central galaxy of the HG is more strongly correlated with the large scale environment in systems with more massive HGs and NNGs.
5. There is a preference for the two major axes of the central galaxies of the HG and NNG to be parallel for the system with the both early central galaxies, while there is no evident correlation between the two major axes of the central galaxies for the systems with both late type central galaxies.
6. Although the distribution of the satellites of the HG is correlated with the direction of the NNG, their orientations (position angles) are not correlated with the direction of the NNG.

According to our various alignment signals measured relative to the direction of the NNG, which is used to represent the large scale environment, we conclude that the distribution of satellite galaxies and the orientations of central galaxies are both affected by or at least correlated with the large scale environment. Such an environmental impact is stronger in massive halos where central galaxies are early type ones. For the orientations of satellite galaxies, however, we did not find any significant alignment signal relative to the direction of NNG, while Faltenbacher et al. (2007) have found prominent alignment signals between the orientations of the central and satellite galaxies at very small separation. This may indicate that the orientations of satellite galaxies are only strongly affected by the tidal force of the central galaxy and the host halo, but not significantly by the large scale environment.

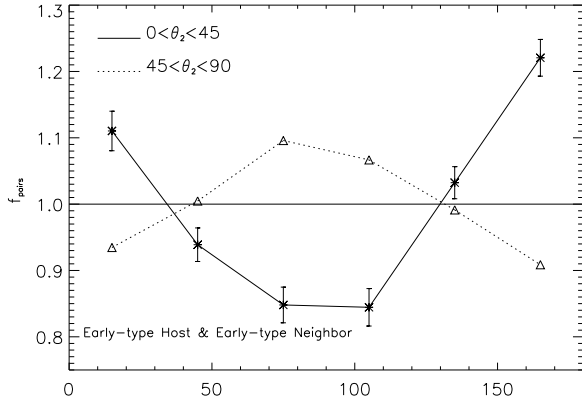


FIG. 15.— The normalized probability distribution, $f_{\text{pairs}}(\theta_1)$, of the angle θ_1 for the systems with early-type host and early-type neighbor. The solid and dotted lines represent the results for the subsamples with $0^\circ < \theta_2 < 45^\circ$ and $45^\circ < \theta_2 < 90^\circ$, respectively.

We have found strong signals in the first and second types of the alignment. Possible explanations for such strong signal are: (i) the large scale environment affects the shape of the host halo, while the distribution of satellite galaxies and the shape of the central galaxy are mainly affected by the host halo; (ii) the large scale environment directly affects the distribution of satellite galaxies and the shape of the central galaxy.

Judging from the first alignment signal, it seems that the impact of large scale environment is mainly on the shape of the host halo instead of directly on the distribution of the satellite galaxies. If the distributions of the satellite galaxies are indeed mainly affected by the NNG directly, we should expect to find a strong dependence on the distance to the NNG, rather than a mass dependence of the HG and NNG.

The fact that stronger alignment signals is found for the subsamples with more massive HGs and NNGs is likely correlated with the fact that the more massive halos have larger triaxialities (e.g. Jing & Suto 2002; Wang & Fan 2004; W08).

In order to check if the shape of the central galaxy is mainly determined/affected by its own host halo, or by the large scale environment, we carried out an additional test. In Figure 15, we show the alignment signal $f_{\text{pairs}}(\theta_1)$ for the systems with the early-type host and early-type neighbor, where the solid and dotted lines show the results for the system with $0^\circ < \theta_2 < 45^\circ$ and $45^\circ < \theta_2 < 90^\circ$, respectively. When $45^\circ < \theta_2 < 90^\circ$, the major axis of the central galaxy of the HG is rather perpendicular to the direction of the NNG. If the shape of central galaxy is not much affected by the host halo, but only affected by the large scale environment, we would expect that the alignment signals of the two subsamples are similar. The results, however, show that the alignment signals are opposite for the two different subsamples. This indicates that the shapes of the central galaxies are quite well correlated with the distributions of the satellite galaxies, hence it is more likely to be determined by their own host halos. This conclusion is

also strengthened by the recent measurements which show that the orientations of the central galaxies are preferentially aligned with the distribution of satellite galaxies (e.g. Y06 and references therein).

Finally, we draw our conclusion that the large scale environment traced by the NNG have impacts on the shape (orientation) of the host halo. On the other hand, the distribution of the satellite galaxies, the shapes of the central galaxies, and the shape of the satellite galaxies at small radii, however, are mainly affected by their own host halos. Apart from these, the NNG also have direct impacts on the distribution of satellite galaxies, which produce an asymmetric alignment signal with respect to the near or far away sides of the NNG.

ACKNOWLEDGMENTS

This work has started during YGW's visit to KIAS. YGW sincerely thank the support of KIAS. CBP and YYC acknowledge the support of the Korea Science and Engineering Foundation (KOSEF) through the Astrophysical Research Center for the Structure and Evolution of the Cosmos (ARCSEC). XY acknowledges the support by the Shanghai Pujiang Program (No. 07pj14102), 973 Program (No. 2007CB815402), the CAS Knowledge Innovation Program (Grant No. KJCX2-YW-T05) and grants from NSFC (Nos. 10533030, 10673023, 10821302). YGW and XLC acknowledges the support of the 973 program (No.2007CB815401), the CAS Knowledge Innovation Program (Grant No. KJCX3-SYW-N2), and the NSFC grant 10503010. XLC is also supported by the NSFC Distinguished Young Scholar Grant No.10525314.

Funding for the SDSS and SDSS-II has been provided by the Alfred P. Sloan Foundation, the Participating Institutions, the National Science Foundation, the U.S. Department of Energy, the National Aeronautics and Space Administration, the Japanese Monbukagakusho, the Max Planck Society, and the Higher Education Funding Council for England. The SDSS Web Site is <http://www.sdss.org/>.

The SDSS is managed by the Astrophysical Research Consortium for the Participating Institutions. The Participating Institutions are the American Museum of Natural History, Astrophysical Institute Potsdam, University of Basel, Cambridge University, Case Western Reserve University, University of Chicago, Drexel University, Fermilab, the Institute for Advanced Study, the Japan Participation Group, Johns Hopkins University, the Joint Institute for Nuclear Astrophysics, the Kavli Institute for Particle Astrophysics and Cosmology, the Korean Scientist Group, the Chinese Academy of Sciences (LAMOST), Los Alamos National Laboratory, the Max-Planck-Institute for Astronomy (MPIA), the Max-Planck-Institute for Astrophysics (MPA), New Mexico State University, Ohio State University, University of Pittsburgh, University of Portsmouth, Princeton University, the United States Naval Observatory, and the University of Washington.

REFERENCES

- Azzaro, M., Patiri, S. G., Prada, F., & Zentner, A. R. 2007, MNRAS, 376, L43
- Bailin, J., & Steinmetz, M. 2005, ApJ, 627, 647
- Basilakos, S., Plionis, M., & Maddox, S. J. 2000, MNRAS, 316, 779
- Binggeli, B. 1982, A&A, 107, 338
- Blanton, M. R., et al. 2005, AJ, 129, 2562
- Brainerd, T. G. 2005, ApJ, 628, L101
- Brainerd, T. G., & Specian, M. A. 2003, ApJ, 593, L7
- Carter, D., & Metcalfe, N. 1980, MNRAS, 191, 325
- Ciotti, L., & Dutta, S. N. 1994, MNRAS, 270, 390
- Dekel, A. 1985, ApJ, 298, 461
- Faltenbacher, A., Li, C., Mao, S., van der Bosch, F. C., Yang, X., Jing, Y. P., Pasquali, A., & Mo, H. J. 2007, ApJ, 662, L71
- Faltenbacher, A., Jing, Y. P., Li, C., Mao, S., Mo, H. J., Pasquali, A., & van den Bosch, F. C. 2008, ApJ, 675, 146
- Fasano, G., Pisani, A., Vio, R., & Girardi, M. 1993, ApJ, 416, 546
- Fleck, J. -J., & Kuhn, J. R. 2003, ApJ, 592, 147
- Hartwick, F. D. A. 1996, in Morrison H., Sarajedini A., eds, ASP Conf. Ser. Vol. 92, Formation of the Galactic Halo . . . Inside and Out. Astron. Soc. Pac., San Francisco, p. 444
- Hartwick, F. D. A. 2000, AJ, 119, 2248
- Hawley, D. L., & Peebles, P. J. E. 1975, AJ, 80, 477
- Holmberg, E. 1969, Ark. Astron., 5, 305
- Jing, Y. P., & Suto, Y. 2002, ApJ, 574, 538
- Kang, X., van den Bosch, F. C., Yang, X., Mao, S., Mo, H. J., Li, C., Jing, Y. P. 2007, MNRAS, 378, 1531
- Katgert, P., Biviano, A., & Mazure, A. 2004, ApJ, 600, 657
- Knebe, A., Draganova, N., Power, C., Yepes, G., Hoffman, Y., Gottlöber, S., & Gibson, B. K. 2008, MNRAS, 386, L52
- Knebe, A., Gill, S. P. D., Gibson, B. K., Lewis, G. F., Ibata, R. A., & Dopita, M. A. 2004, ApJ, 603, 7
- Koch, A., & Grebel, E. K. 2006, AJ, 131, 1405
- Kroupa, P., Theis, C., & Boily, C. M. 2005, A&A, 431, 517
- Libeskind, N. I., Frenk, C. S., Cole, S., Helly, J. C., Jenkins, A., Navarro, J. F., & Power, C. 2005, MNRAS, 363, 146
- Lynden-Bell, D. 1976, MNRAS, 174, 695
- Lynden-Bell, D. 1982, Observatory, 102, 202
- MacGillivray, H. T., Dodd, R. J., McNally, B. V., & Corwin H. G. Jr. 1982, MNRAS, 198, 605
- Majewski, S. R. 1994, ApJ, 431, L17
- McConnachie, A. W., & Irwin, M. J. 2006, MNRAS, 365, 902
- McKay, T., et al. 2002, ApJ, 571, L85
- Metz, M., Kroupa, P., & Jerjen, H., 2007, MNRAS, 374, 1125
- Orlov, V. V., Petrova, A. V., & Tarantsev, V. G. 2001, MNRAS, 325, 133
- Park, C., & Choi, Y.-Y. 2005, ApJ, 635, L29
- Plionis, M. 1994, ApJS, 95, 401
- Plionis, M., Barrow, J. D., & Frenk C. S. 1991, MNRAS, 249, 662
- Plionis, M., Basilakos, S., & Tovmassian, H. M. 2004, MNRAS, 352, 1323
- Plionis, M., Barrow, J. D., & Frenk, C. S. 1991, MNRAS, 249, 662
- Plionis, M., Benoist, C., Maurogordato, S., Ferrari, C., & Basilakos, S. 2003, ApJ, 594, 144
- Porciani, C., Dekel, A., & Hoffman, Y. 2002, MNRAS, 332, 325
- Sharp, N. A., Lin, D. N. C., & White S. D. M., 1979, MNRAS, 187, 287
- Steffen, J. H., & Valenzuela, O. 2008, MNRAS, 387, 1199
- Strazzullo, V., Paolillo, M., Longo, G., Puddu, E., Djorgovski, S. G., De Carvalho, R. R., & Gal, R. R. 2005, MNRAS, 359, 191
- Struble, M. F. 1990, AJ, 99, 743
- Torlina, L., De Propriis, R., & West, M. J. 2007, ApJ, 660, L97
- Usami, M., & Fujimoto, M. 1997, ApJ, 487, 489
- van den Bosch, F. C., Norberg, P., Mo, H. J., & Yang, X. 2004, MNRAS, 352, 1302
- Wang, H. Y., Jing, Y. P., Mao, S., & Kang, X. 2005, MNRAS, 364, 424
- Wang, Y.-G., & Fan, Z.-H. 2004, ApJ, 617, 847
- Wang, Y., Yang, X., Mo, H. J., Li, C., van den Bosch, F. C., Fan, Z., & Chen, X. 2008, MNRAS, 385, 1511 (W08)
- West, M. J. 1989, ApJ, 344, 535
- West, M. J. 1994, MNRAS, 268, 79
- Yang, X., Mo, H. J., van den Bosch, F. C., & Jing, Y. P. 2005, MNRAS, 356, 1293
- Yang, X., van der Bosch, F. C., Mo, H. J., Mao, S., Kang, X., Weinmann, S. M., Guo, Y., & Jing, Y. P., 2006, MNRAS, 369, 1293 (Y06)
- Yang X., Mo H.J., van den Bosch F.C., Pasquali A., Li C., Barden M., 2007, ApJ, 671, 153
- Yang X., Mo H.J., van den Bosch F.C., 2008, preprint, arXiv:0808.0539
- Zaritsky, D., Smith, R., Frenk, C. S., & White, S. D. M. 1993, ApJ, 405, 464
- Zaritsky, D., Smith, R., Frenk, C. S., & White, S. D. M. 1997, ApJ, 478, 39
- Zehavi, I., et al. 2002, ApJ, 571, 172
- Zentner, A. R., Kravtsov A. V., Gnedin, O. Y., Klypin, A. A. 2005, ApJ, 629, 219

6. APPENDIX

In this appendix, we will explain how to get the angle between the orientation of the central galaxy of the host group and NN. We take one pair of the host $(\alpha_h, \delta_h, \Phi_h)$ and neighbor $(\alpha_n, \delta_n, \Phi_n)$ as an example, where α_h , δ_h and Φ_h are the right ascension, declination, and the position angle of the host centrals respectively, and α_n , δ_n and δ_n are the corresponding parameters of the NN. Here we assume that $\alpha_n > \alpha_h$, $\delta_h > 0$, and $\delta_n > 0$ (See the right panel of Figure 2). Extending the major axis of the central galaxy of the NN, it will cross the longitude of the host at the point B. Now in the spherical triangle $\triangle ABC$, we have two angles $\angle BAC$ and $\angle ACB$ and one side \widehat{AC} . Therefore, we can get the angle $\angle CBA$ by solving the spherical triangle $\triangle ABC$. It is clear that the angle between the orientation of the central galaxy of the host group and NN can be written as $\Phi_h - (180^\circ - \angle CBA)$, which is equivalent to the angle $\theta_3 = \theta_{3a} - \theta_{3b}$ (see the right panel of Figure 2). Position angles of the major axes are with respect to the east direction.